# ChemComm

Chemical Communications

rsc.li/chemcomm

ROYAL SOCIETY OF CHEMISTRY | Celebrating IYPT 2019

**COMMUNICATION**
Seung Uk Son *et al.*
Nanoparticulate and microporous solid acid catalysts
bearing aliphatic sulfonic acids for biomass conversion

# ChemComm

Check for updates

## Nanoparticulate and microporous solid acid catalysts bearing aliphatic sulfonic acids for biomass conversion†

Kyoungil Cho,[a] Sang Moon Lee,[b] Hae Jin Kim,[b] Yoon-Joo Ko[c] and Seung Uk Son (ID) *[a]

This work introduces new nanocatalytic systems based on micro-porous organic network (MON) chemistry for fructose conversion to 5-hydroxymethylfurfural (HMF). The efficiency of the catalytic systems could be improved through the size-controlled synthesis of MON materials. Through a predesigned building block approach and a post-synthetic modification, aliphatic sulfonic acid groups were incorporated into nano-sized MON materials to form N-MON-AS. The N-MON-AS showed selective conversion of fructose to HMF in up to 91% yield at 100 °C and good recyclability.

Plants are sustainable chemical resources to replace depletable petroleum.[1] Carbohydrates such as cellulose and hemicelluloses in the cell walls of plants can be converted to monosaccharides such as glucose and fructose.[1] The monosaccharides can be ultimately converted to a furan derivative, 5-hydroxymethylfurfural (HMF). As a sustainable starting material, HMF has been utilized for the chemical synthesis of various functional compounds and polymers.[2] Thus, HMF is one of the most important compounds to proceed furan-based sustainable chemistry, the so-called furanics.[3]

In the last decade, there have been extensive studies on the conversion of monosaccharides to HMF.[4] The Brønsted acids have been used to catalyze the conversion of monosaccharides to HMF. For example, sulfuric acid catalyzes the abstraction of three waters from each monosaccharide to form HMF. To be a more practical chemical process, solid acids with sulfonic acid groups have been utilized.[5] Conventional solid acids have been engineered on micron-sized supports.[5] As far as we are aware, nano-sized solid acids have rarely been studied[6] and more

studies are required to improve the catalytic performance of solid acids.

Recently, porous polymer-based solid acids have been developed to utilize inner Brønsted acid sites.[7] For example, microporous organic network (MON)-based solid sulfonic acids with high surface areas, microporosity, and chemical stability have been developed.[7] However, the catalytic performance of MON-based catalysts is dependent on the size of MON particles because substrates have to be diffused into MON materials to react with the inner catalytic sites. Moreover, the diffusion pathways can be easily clogged by substrates or products. Thus, the size control of MON particles may be critical to improve the catalytic performance of MON-based solid acids.

Recently, there has been much progress in the nanoengineering of organic and inorganic polymeric materials.[8] In particular, the kinetic growth control of polymeric materials using surfactants has shown many successful results.[8] In this regard, nano-sized MON materials have also been developed using surfactants.[8] In this work, we report the engineering of nano-sized MON-based solid acids bearing sulfonic acids and their improved catalytic performance in the chemical conversion of fructose to HMF.

Fig. 1 shows the synthetic schemes of conventional micron-sized MON materials and nano-sized MON particles and their post-synthetic modification to incorporate aliphatic sulfonic acid (AS) groups. Conventional micron-sized MON materials were prepared by the Sonogashira coupling of tetra(4-ethynylphenyl)-adamantane with 1,4-dibromo-2,5-di(trimethylsilylethynyl)benzene. In the presence of poly(vinylpyrrolidone) (PVP), nano-sized MON particles were prepared. In the work-up process, treating the nano-sized MON particles with HF solution resulted in nano-sized MON particles with terminal alkyne groups (N-MON). Through the thiol–yne click reaction,[9] sodium sulfonate groups were incorporated into the N-MON particles. Treating the nano-sized MON particles bearing sodium sulfonate groups with sulfuric acid resulted in nano-sized MON particles bearing aliphatic sulfonic acids (N-MON-AS). As a control material, conventional micron-sized MON materials bearing aliphatic sulfonic acids (MON-AS) were prepared without using the PVP surfactant.

[a] *Department of Chemistry, Sungkyunkwan University, Suwon 16419, Korea.*
  *E-mail: sson@skku.edu*
[b] *Korea Basic Science Institute, Daejeon 34133, Korea*
[c] *Laboratory of Nuclear Magnetic Resonance, National Center for Inter-University Research Facilities (NCIRF), Seoul National University, Seoul 08826, Korea*

† Electronic supplementary information (ESI) available: Experimental procedures, and additional characterization data of N-MON-AS and MON-AS. See DOI: 10.1039/c9cc00436j
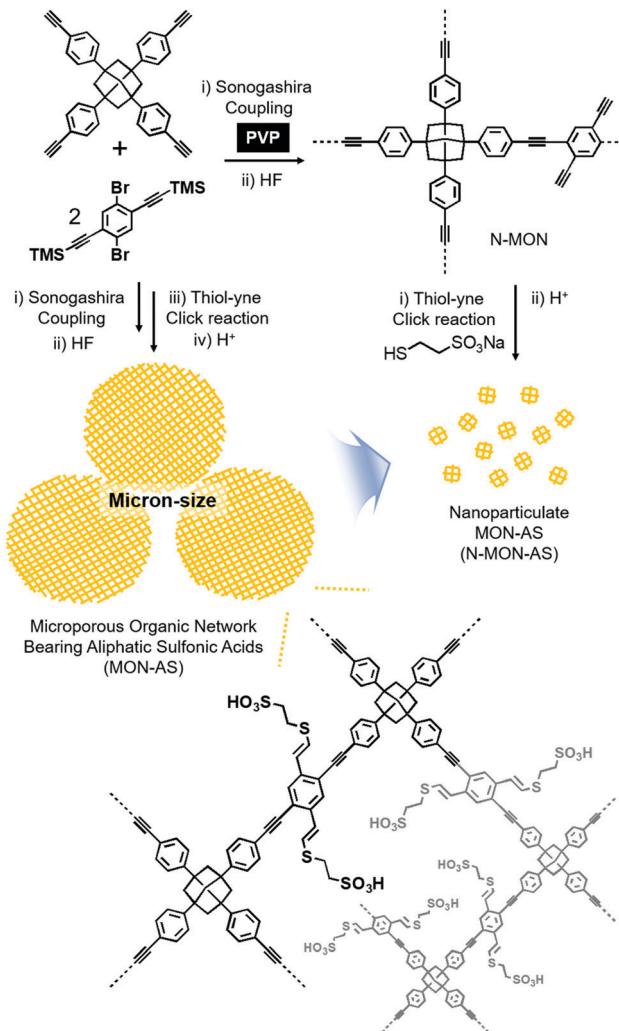
Fig. 1 Synthesis of a micron-sized microporous organic network bearing aliphatic sulfonic acids (MON-AS) and nanoparticulate MON-AS (N-MON-AS).



Fig. 2 SEM images of (a and d) MON-AS, (b and e) N-MON, and (c) N-MON-AS. (f) TEM image of N-MON-AS. TEM-EDS elemental mapping images of (g) MON-AS and (h) N-MON-AS.

The morphologies and sizes of MON materials were investigated by scanning (SEM) and transmission electron microscopy (TEM). As shown in Fig. 2a and d, the SEM images of MON materials prepared without using PVP surfactant showed micron-sized spheres with diameters of $1.3 \pm 0.3$ μm and a relatively broad size distribution (Fig. S1 in the ESI†). In contrast, the MON materials prepared in the presence of PVP showed nano-sized particles with an average diameter of $97 \pm 11$ nm and a narrow size distribution (Fig. 2b, e and Fig. S1 in the ESI†). To achieve the monodisperse size distribution, we scanned the amount of PVP in the synthesis of N-MON materials (Fig. S2 in the ESI†). As the amount of PVP increased, the size uniformity of MON materials was improved. The N-MON-AS maintained the original morphologies of N-MON materials (Fig. 2c and f). Elemental mapping based on energy dispersive X-ray spectroscopy (EDS) indicated the homogeneous distribution of sulfonic acids in the MON-AS and N-MON-AS (Fig. 2g and h).

The physical and chemical properties of MON materials were further characterized by various analysis methods (Fig. 3). The N₂ adsorption–desorption isotherm curves (77 K) of MON materials

were analyzed based on the Brunauer–Emmett–Teller theory. The micron-sized MON and MON-AS showed surface areas of 563 and 453 m² g⁻¹ with micropore volumes of 0.18 and 0.13 cm³ g⁻¹, respectively (Fig. 3a). The decreased surface area and micropore volume of MON-AS are attributable to the incorporated additional sulfonic acid groups in the materials, matching well with the conventional trends reported in the literature.[10] Similarly, the N-MON and N-MON-AS showed surface areas of 609 and 546 m² g⁻¹ and micropore volumes of 0.19 and 0.17 cm³ g⁻¹, respectively (Fig. 3b). The analysis of the pore size distributions based on the density functional theory method revealed that all the MON materials have microporosity (pore sizes < 2 nm) (Fig. 3a and b). Powder X-ray and electron diffraction studies revealed that all the MON materials have amorphous inner structures, which is a conventional feature of the MON materials prepared by Sonogashira coupling in the literature[11] (Fig. S3 in the ESI†).

The infrared (IR) absorption spectra of all MON materials showed aromatic C–H and C═C vibration peaks at 830 and 1603 cm⁻¹, respectively, and aliphatic C–H vibration peaks at 3925–2840 and 1493 cm⁻¹, indicating that the MON materials were formed through the coupling of the used adamantane building blocks (Fig. 3c and d). In the IR absorption spectra of N-MON and N-MON-AS, additional C═O vibration peaks were observed at 1660 cm⁻¹, corresponding to the entrapped PVP in the MON networks (Fig. 3d).

After the post-synthetic modification of MON and N-MON materials with sulfonic acid moieties, new vibration peaks appeared at 1200 and 3445 cm⁻¹, corresponding to S═O and
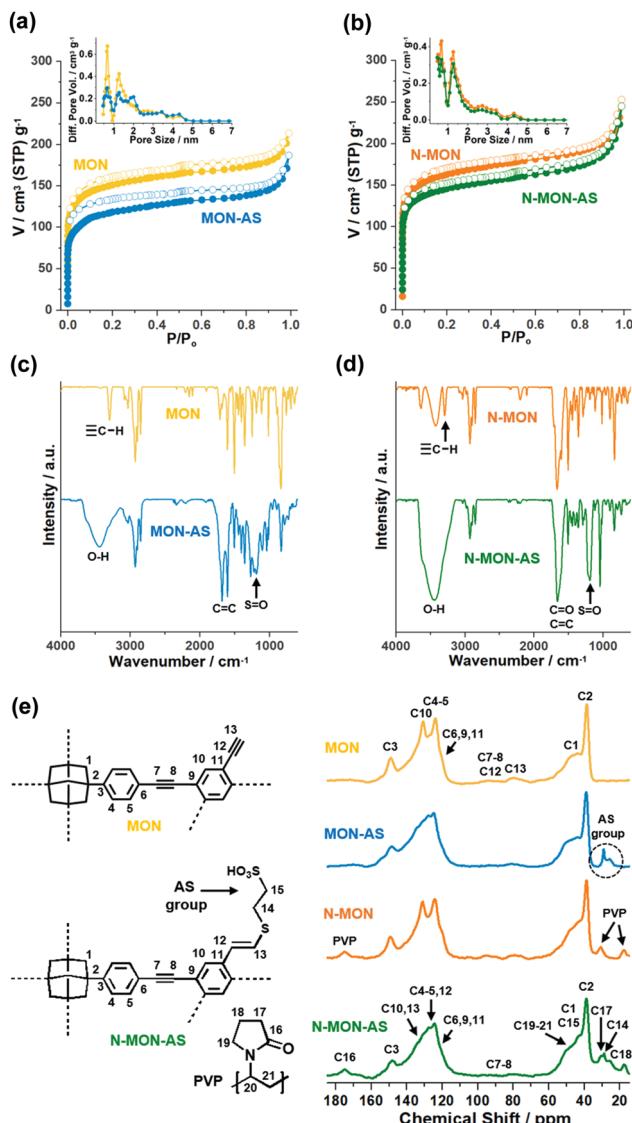
Fig. 3 (a and b) $N_2$ adsorption–desorption isotherm curves obtained at 77 K and pore size distribution diagrams based on the density functional theory (DFT) method, (c and d) IR absorption, and (e) solid state $^{13}C$ NMR spectra of MON, MON-AS, N-MON, and N-MON-AS.

OH vibrations of sulfonic acid groups (Fig. 3c and d). In addition, new alkene C=C vibration peaks appeared at 1683 cm$^{-1}$, indicating that the sulfonic acid moieties were introduced to alkynes *via* a thiol–yne click reaction. In the IR absorption spectra of MON and N-MON materials, both internal and terminal alkyne peaks were observed at 2210 and 2150–2100 cm$^{-1}$, respectively. Moreover, C–H vibrations of terminal alkynes were observed at 3295 cm$^{-1}$. In comparison, in the IR absorption spectra of MON-AS and N-MON-AS, the terminal alkyne peaks at 2150–2100 and 3295 cm$^{-1}$ disappeared, indicating that the sulfonic acid moieties were introduced through the thiol–yne click reaction of terminal alkynes.

The solid state nuclear magnetic resonance (NMR) spectra of all MON materials showed adamantane $^{13}C$ peaks at 39 and 46 ppm. The MON and N-MON showed aromatic $^{13}C$ peaks at 124, 131, and 149 ppm, in addition to terminal and internal

alkyne $^{13}C$ peaks at 80 and 93 ppm, respectively (Fig. 3e). The N-MON and N-MON-AS showed additional $^{13}C$ peaks at 17, 31, and 175 ppm, corresponding to the alkyl and carbonyl groups of the entrapped PVP. In the $^{13}C$ NMR spectra of MON-AS and N-MON-AS, the $^{13}C$ peaks of alkynes were weakened and the aromatic $^{13}C$ peaks were significantly changed. Moreover, new $^{13}C$ peaks appeared at 26–29 ppm, corresponding to the aliphatic sulfonic groups. According to acid–base titration, the contents of effective sulfonic acids in the MON-AS and N-MON-AS were measured to be 0.284 and 0.731 mmol g$^{-1}$, respectively. Thermogravimetric analysis showed that the MON-AS and N-MON-AS are stable up to ∼216 and ∼225 °C, respectively (Fig. S4 in the ESI†).

Solid acids with sulfonic acids have been utilized in various organic reactions.[12] Recently, as research interest in sustainable chemistry has increased, fructose conversion to HMF has become one of the most important reactions[1] (Fig. 4a). Solid acid catalysts can improve HMF selectivity at low temperature. Considering the nanosize and porosity of N-MON-AS, we studied its catalytic performance in fructose conversion to HMF. Fig. 4 and Fig. S5 in the ESI† summarize the results.

As shown in Fig. 4b, N-MON-AS with 2 mol% sulfonic acids showed 98, 96, and 91% yields of HMF after 20 h at 140, 120, and 100 °C, respectively. At 80 and 60 °C, the HMF yields were
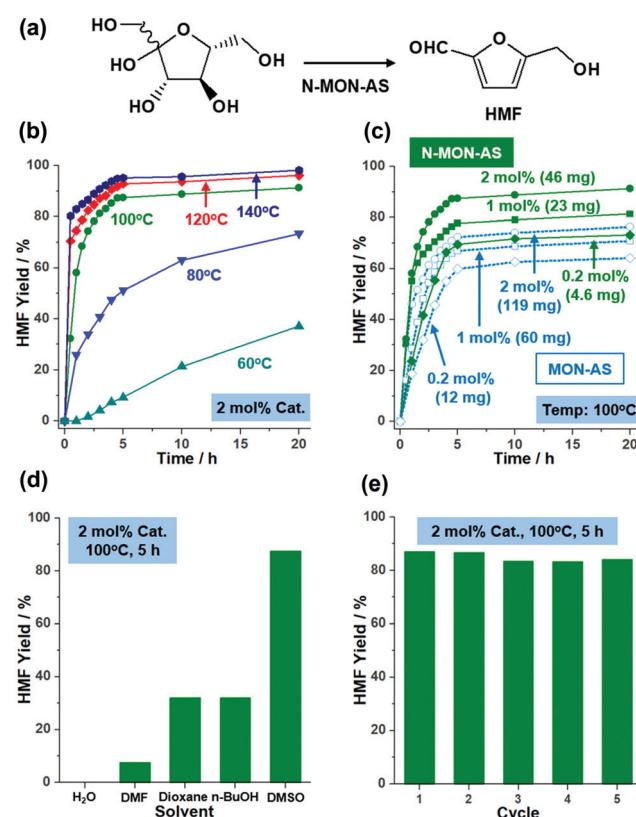


Fig. 4 (a) A scheme of fructose conversion to HMF. (b) Temperature-dependent catalytic performance of N-MON-AS. (c) Comparison of the catalytic performance of MON-AS (0.284 mmol SO$_3$H per g) and N-MON-AS (0.731 mmol SO$_3$H per g). (d) Solvent-dependent catalytic performance and (e) recyclability of N-MON-AS.

reduced to 73 and 37%, respectively. In the literature,[5,7a] the conversion of fructose to HMF has usually been studied at a high temperature of > 120 °C. It is noteworthy that the N-MON-AS significantly retained catalytic activity at 100 °C with an HMF yield of 91%. Moreover, when we reduced the amount of N-MON-AS to 1 and 0.2 mol% at 100 °C, HMF yields of 81 and 73% were obtained, respectively, corresponding to a turn over number (TON) of 81 and 365, respectively (Fig. 4c). In comparison, micron-sized MON-AS with 0.2, 1, and 2 mol% sulfonic acids showed HMF yields of 64, 71, and 76% at 100 °C, indicating that the relatively slow reaction induced side reactions and resulted in decreased HMF selectivity due to the elongated diffusion pathways of the substrate[13] in the micron-sized MON-AS. It is also noteworthy that a much greater weight of MON-AS by 2.6 times had to be used for the same mol% $SO_3H$ in the solid acid catalysts, compared with those of N-MON-AS.

Recently, sulfonated MON-based catalysts have been prepared in the literature[7a] and show catalytic activities in the conversion of fructose to HMF with TONs of 5.83 and 6.11 at 120 and 140 °C, respectively. In addition, the catalytic performance of N-MON-AS in this work is superior to hollow sulfonated MON catalysts[7g] with a diameter of 300 nm and a surface area of 387 m² g⁻¹ showing TONs of 42.5 and 45.5 at 100 and 120 °C, respectively. The promising catalytic performance (TONs of 81–365 at 100 °C) of N-MON-AS is attributable to its reduced size (97 ± 11 nm) and a higher surface area (503 m² g⁻¹).

When we scanned solvent systems, we could not obtain HMF in water because excess water can suppress the water abstraction from fructose (Fig. 4d). In dimethylformamide, a poor HMF yield of 7.6% was observed with the unreacted fructose after 5 h at 100 °C because the basic nature of DMF hindered the Brønsted acid catalytic action of N-MON-AS. In the case of BuOH and 1,4-dioxane, although the fructose was completely converted, both yields of HMF were 32% after 5 h at 100 °C. The N-MON-AS could be recycled at least five times, maintaining 100, 96, 96, and 97% of the original catalytic activity at the second, third, fourth, and fifth cycles, respectively (Fig. 4e). The SEM and $N_2$ sorption isotherm analysis of the recovered N-MON-AS after the recycling tests showed the retention of the original morphologies of the materials and a surface area of 558 m² g⁻¹ (Fig. S6 in the ESI†).

In conclusion, nano-sized solid acid catalysts with diameters in the range of 90–100 nm were developed through the size-controlled synthesis of MON materials in the presence of PVP surfactants. After introducing terminal alkynes into the materials through a predesigned building block approach, the aliphatic sulfonic acid groups were incorporated into the nano-sized MON materials through a post-synthetic modification approach. The obtained N-MON-AS showed not only promising catalytic activities in fructose conversion to HMF at 100 °C but also good recyclability

in the five successive recycling tests. We believe that the nano-sized solid acid catalysts of this work can be utilized for the various organic conversions that have been conducted with micron-sized solid acids.[12]

## Conflicts of interest

There are no conflicts to declare.

## Notes and references

1 H. Zhu, W. Luo, P. N. Ciesielski, Z. Fang, J. Y. Zhu, G. Henriksson, M. E. Himmel and L. Hu, *Chem. Rev.*, 2016, **116**, 9305–9374.
2 (a) Y. Nakagawa, M. Tamura and K. Tomishige, *ACS Catal.*, 2013, **3**, 2655–2668; (b) M. E. Zakrzewska, E. Bogel-Łukasik and R. Bogel-Łukasik, *Chem. Rev.*, 2011, **111**, 397–417.
3 B. R. Caes, R. E. Teixeira, K. G. Knapp and R. T. Raines, *ACS Sustainable Chem. Eng.*, 2015, **3**, 2591–2605.
4 B. Liu and Z. Zhang, *ACS Catal.*, 2016, **6**, 326–338.
5 (a) M. Hara, *Energy Environ. Sci.*, 2010, **3**, 601–607; (b) Z.-Z. Yang, J. Deng, T. Pan, Q.-X. Guo and Y. Fu, *Green Chem.*, 2012, **14**, 2986–2989.
6 L. Wang and F.-S. Xiao, *Green Chem.*, 2015, **17**, 24–39.
7 (a) S. Mondal, J. Mondal and A. Bhaumik, *ChemCatChem*, 2015, **7**, 3570–3578; (b) S. Bhunia, B. Banerjee and A. Bhaumik, *Chem. Commun.*, 2015, **51**, 5020–5023; (c) M. M. Islam, S. Bhunia, R. A. Molla, A. Bhaumik and S. M. Islam, *ChemistrySelect*, 2016, **1**, 6079–6085; (d) F. Liu, Q. Wu, C. Liu, C. Qi, K. Huang, A. Zheng and S. Dai, *ChemSusChem*, 2016, **9**, 2496–2504; (e) C. Klumpen, S. Gödrich, G. Papastavrou and J. Senker, *Chem. Commun.*, 2017, **53**, 7592–7595; (f) S. Mondal, B. C. Patra and A. Bhaumik, *ChemCatChem*, 2017, **9**, 1469–1475; (g) K. Cho, S. M. Lee, H. J. Kim, Y.-J. Ko and S. U. Son, *J. Mater. Chem. A*, 2018, **6**, 15553–15557.
8 (a) A. Patra, J.-M. Koenen and U. Scherf, *Chem. Commun.*, 2011, **47**, 9612–9614; (b) K. Wu, J. Guo and C. Wang, *Chem. Commun.*, 2014, **50**, 695–697; (c) B. C. Ma, S. Ghasimi, K. Landfester, F. Vilela and K. A. I. Zhang, *J. Mater. Chem. A*, 2015, **3**, 16064–16071; (d) P. Pallavi, S. Bandyopadhyay, J. Louis, A. Deshmukh and A. Patra, *Chem. Commun.*, 2017, **53**, 1257–1260; (e) B. H. Lee, K. C. Ko, J. H. Ko, S. Y. Kang, S. M. Lee, H. J. Kim, Y.-J. Ko, J. Y. Lee and S. U. Son, *ACS Macro Lett.*, 2018, **7**, 651–655.
9 B. Kiskan and J. Weber, *ACS Macro Lett.*, 2012, **1**, 37–400.
10 (a) H. Urakami, K. Zhang and F. Vilela, *Chem. Commun.*, 2013, **49**, 2353; (b) T. İslamoğlu, M. G. Rabbani and H. M. El-Kaderi, *J. Mater. Chem. A*, 2013, **1**, 10259–10266; (c) N. Park, Y. N. Lim, S. Y. Kang, S. M. Lee, H. J. Kim, Y.-J. Ko, B. Y. Lee, H.-Y. Jang and S. U. Son, *ACS Macro Lett.*, 2016, **5**, 1322–1326; (d) J. Choi, E. S. Kim, J. H. Ko, S. M. Lee, H. J. Kim, Y.-J. Ko and S. U. Son, *Chem. Commun.*, 2017, **53**, 8778–8781.
11 J.-X. Jiang, F. Su, A. Trewin, C. D. Wood, N. L. Campbell, H. Niu, C. Dickinson, A. Y. Ganin, M. J. Rosseinsky, Y. Z. Khimyak and A. I. Cooper, *Angew. Chem., Int. Ed.*, 2007, **46**, 8574–8578.
12 P. Gupa and S. Paul, *Catal. Today*, 2014, **236**, 152–170.
13 (a) J. H. Ko, N. Kang, N. Park, H.-W. Shin, S. Kang, S. M. Lee, H. J. Kim, T. K. Ahn and S. U. Son, *ACS Macro Lett.*, 2015, **4**, 669–672; (b) K. Cho, J. Yoo, H.-W. Noh, S. M. Lee, H. J. Kim, Y.-J. Ko, H.-Y. Jang and S. U. Son, *J. Mater. Chem. A*, 2017, **5**, 8922–8926.